# Theoretical and experimental study of the flow of a molten polymer in a micro-compounder

Irène Berton, Romain Castellani, Lucas Sardo, Rudy Valette, Bruno Vergnes

# Theoretical and experimental study of the flow of a molten polymer in a micro-compounder

Irène Berton[1], Romain Castellani[1], Lucas Sardo[2], Rudy Valette[1], Bruno Vergnes[1]

[1] MINES ParisTech, PSL Research University, CEMEF, UMR CNRS 7635, CS 10207, 06904 Sophia Antipolis (France)

[2] Sciences Computers Consultants, 42000, Saint Etienne (France)

**Abstract**

Micro-compounders are more and more used to characterize and optimize the formulations and the flow conditions of complex materials, with very low quantities, around a few grams. These machines are composed of a small-size conical twin-screw extruder, coupled with a recirculating channel, in which the material can be processed during a fixed time and a certain number of cycles, before being purged. However, the precise flow conditions inside these machines are not well known, what makes an optimal interpretation of the results difficult. Therefore, in this paper, a theoretical model based on continuum mechanics is proposed to calculate the flow in the recirculating mode. An experimental study on a well-chosen polymer is carried out to define the influences of the main processing parameters (screw speed, mass of material, barrel temperature) and to validate the model. Despite the simplicity of the theoretical approach, the calculated results are in satisfactory agreement with the experiments.

**Keywords**: micro-compounder, twin-screw extrusion, molten polymer, flow modelling,

Corresponding author: Bruno Vergnes

bruno.vergnes@mines-paristech.fr

+33 493 95 74 63

## 1 INTRODUCTION

Mixing and compounding of polymers are an essential part of the polymer industry. At an industrial level, these operations are generally carried out using twin-screw extruders, able to provide flow rates up to tens of tons per hour. However, to develop a product at the lab scale, smaller machines are necessary. Twin-screw extruders with a diameter as low as 11 mm are now available on the market. However, for expensive materials or available in very low amounts, flow rates of a few grams per hour would be desirable, at least to define appropriate formulations. Therefore, at the end of the nineties, a new class of machines appeared, called micro-compounders. Developed by several companies (ThermoFisher with Haake Minilab, DSM with Xplore, DACA), they are based on the same idea: coupling a small-size twin-screw extruder (either co- or counterrotating) with a recirculating channel. The material can thus be processed with the necessary residence time, but in real extrusion conditions. Once this treatment is achieved, a valve allows to purge the material by extruding it through a die. On some machines, the design of the recirculating channel also allows to deduce an apparent viscosity from the measurement of the local pressure drop.

In the literature, micro-compounders have been used for various applications, for example the dispersion of PP/PS blends [1], the manufacturing of nanocomposites (PS/PA6/kaolin [2], PS/graphene [3], polycarbonate/carbon nanotubes [4], PA6/organoclay [5]), the modification of LDPE. [6] They are also more and more used for pharmaceutical applications, where the ingredients of the formulations are often very expensive. [7-11] However, despite this increasing use, there are few scientific approaches to the process itself.

An example concerns the use of a micro-compounder of Haake type for rheological measurements. The pressure drop in the recirculating channel, measured by two flush-mounted pressure sensors, provides the value of the shear stress. But the shear rate must be obtained from the flow rate, which is a priori unknown. Indeed, it results from the equilibrium between the

pressure created by the extruder and that consumed in the recirculating channel and cannot be imposed by the user. In the previous users' manuals, it was indicated that the volume flow rate $Q_v$ was proportional to the screw rotation speed $N$:

$$Q_v = C\,N \tag{1}$$

where $C$ was a constant, independent of the polymer and the configuration (co- or counter-rotating), and equal to 0.0133 for $N$ expressed in rpm and $Q_v$ in $cm^3/s$. By carefully measuring the flow rate in various flow conditions and for different materials, Yousfi et al. [12] demonstrated that this value was largely overestimated and that values in the range $5.5\ 10^{-4}$ – $10.7\ 10^{-4}$ were more realistic. Moreover, this coefficient was dependent on polymer viscosity and temperature. A value of $6.0\ 10^{-4}$, but identical for two temperatures, was also proposed by Decaen et al. [13]. In more recent users' manuals, Haake proposes now to differentiate co- and counter-rotating configurations and to include the pressure $P_1$ at the entry of the measuring channel. For a co-rotating system, the flow rate is now defined as:

$$Q_v = C^*\,N\,P_1^{-0.1} \tag{2}$$

with $C^* = 9.17\ 10^{-4}$ for $P_1$ expressed in Pa. This allows to take indirectly into account the effects of viscosity and temperature.

This example shows the lack of scientific understanding of the behavior of micro-compounders. Indeed, to our knowledge, no modelling approach exists in the literature and the experimental studies are seldom. Sakai and Thommes [14] showed that the temperature at different locations of the barrel was uniform and that the specific mechanical energy (SME) increased non-linearly with the screw speed and linearly with the recirculation time. Wang et al. [15] reported that the torque increased non-linearly with the screw speed and studied the effect of the quantity of material introduced in the micro-compounder. At constant screw speed, the torque increased linearly with the feeding quantity, until reaching a plateau above a quantity that depended on

the polymer used. This limit was independent of the screw speed and corresponded to a total filling of the micro-compounder.

The objectives of the present work are to understand more accurately the behavior of a molten polymer during the recirculation into a micro-compounder. An experimental study is first carried out, followed by an analytical modelling of the process and a comparison between the experiments and the results of the model.

## 2 EXPERIMENTAL STUDY

### 2.1 Materials and methods

A micro-compounder Haake Minilab has been selected for the study. The free volume of the machine is around 7 mL. The scheme of the machine is shown in Figure 1. It is composed of a conical twin-screw extruder (A), coupled with a recirculating channel (B). A valve (C) allows to purge the material through the die (D) once the recirculation is achieved. It can be operated either in co- or counter-rotating mode. In the present study, we focus only on the co-rotating configuration shown in Figure 1. Two pressure transducers ($P_1$ and $P_2$) are flush-mounted at the extremities of the recirculating channel (B) to estimate the melt viscosity. The main dimensions of the micro-compounder, directly measured on the machine, are indicated in Table 1.

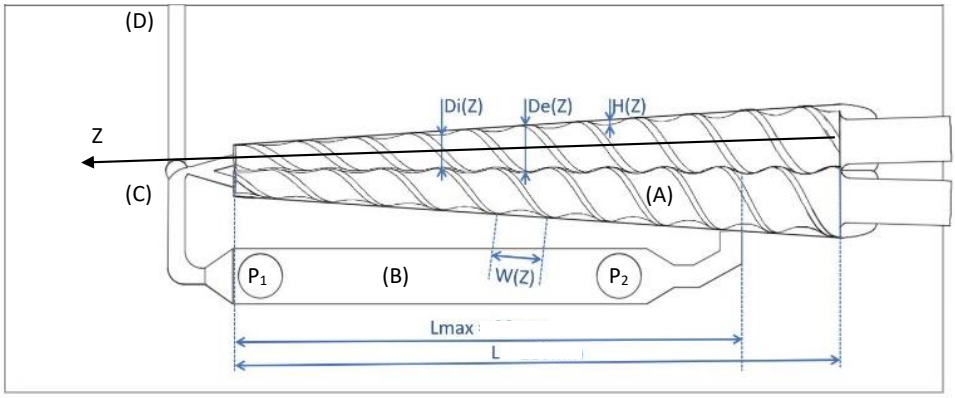


Figure 1. Schematic representation of the Haake Minilab micro-compounder. The circles in channel (B) indicate the location of the pressure transducers.

Table 1. Main dimensions of the micro-compounder. All values are in mm.

| | | |
|---|---|---|
| Initial external screw diameter | $D_{0e}$ | 14 |
| Initial internal screw diameter | $D_{0i}$ | 10 |
| Final external screw diameter | $D_{1e}$ | 5 |
| Final internal screw diameter | $D_{1i}$ | 4 |
| Screw length | $L$ | 109.5 |
| Flight thickness | $e$ | 1 |
| Screw pitch | $B$ | 25 |
| Screw length between tip and channel exit | $L_{max}$ | 90 |
| Length of the recirculating channel | $L_3$ | 75 |
| Width of the recirculating channel | $w_3$ | 10 |
| Depth of the recirculating channel | $h_3$ | 1.5 |
| Length of the junction channel between (C) and (B) | $L_2$ | 24 |
| Width of the junction channel between (C) and (B) | $w_2$ | 3 |
| Depth of the junction channel between (C) and (B) | $h_2$ | 3 |
| Length of the junction channel between (B) and (A) | $L_4$ | 15 |
| Width of the junction channel between (B) and (A) | $w_4$ | 4 |
| Depth of the junction channel between (B) and (A) | $h_4$ | 1.5 |

The polymer selected for the study is a polypropylene homopolymer (PPH5060, provided by Total). It has a melt-index of 6 g/10 min (230°C, 2.16 kg) and a melt density of 0.734 g/cm$^3$. [16] Its rheological behavior can be described by a Carreau-Yasuda law, with the following parameters (at 200°C): Newtonian viscosity $\eta_0$ = 4810 Pa.s, characteristic time, $\lambda$ = 0.21 s, Yasuda parameter $a$ = 0.53, power law index $n$ = 0.34, activation energy $E$ = 39.8 kJ/mol.

### 2.2 Experimental results

Measurements have been carried out during the recirculation and the purge, by varying screw speed ($N$ = 100-200 rpm), barrel temperature ($T_b$ = 180-220°C) and feed mass ($m$ = 2-5 g). With the selected polymer, 2 g is not enough to fill the recirculating channel and 5 g leads to a complete filling. For each condition, the melt temperature, the torque, the mechanical energy, the pressures of the two transducers, and the flow rate during the purge have been recorded.

### *2.2.1 Melt temperature*

The temperature has been measured by introducing a manual thermocouple into the melt through the hopper, after having stopped the screw rotation. As shown in Figure 2a, the melt temperature increases linearly with the barrel temperature, and is not very sensitive to the screw speed, in the tested range.

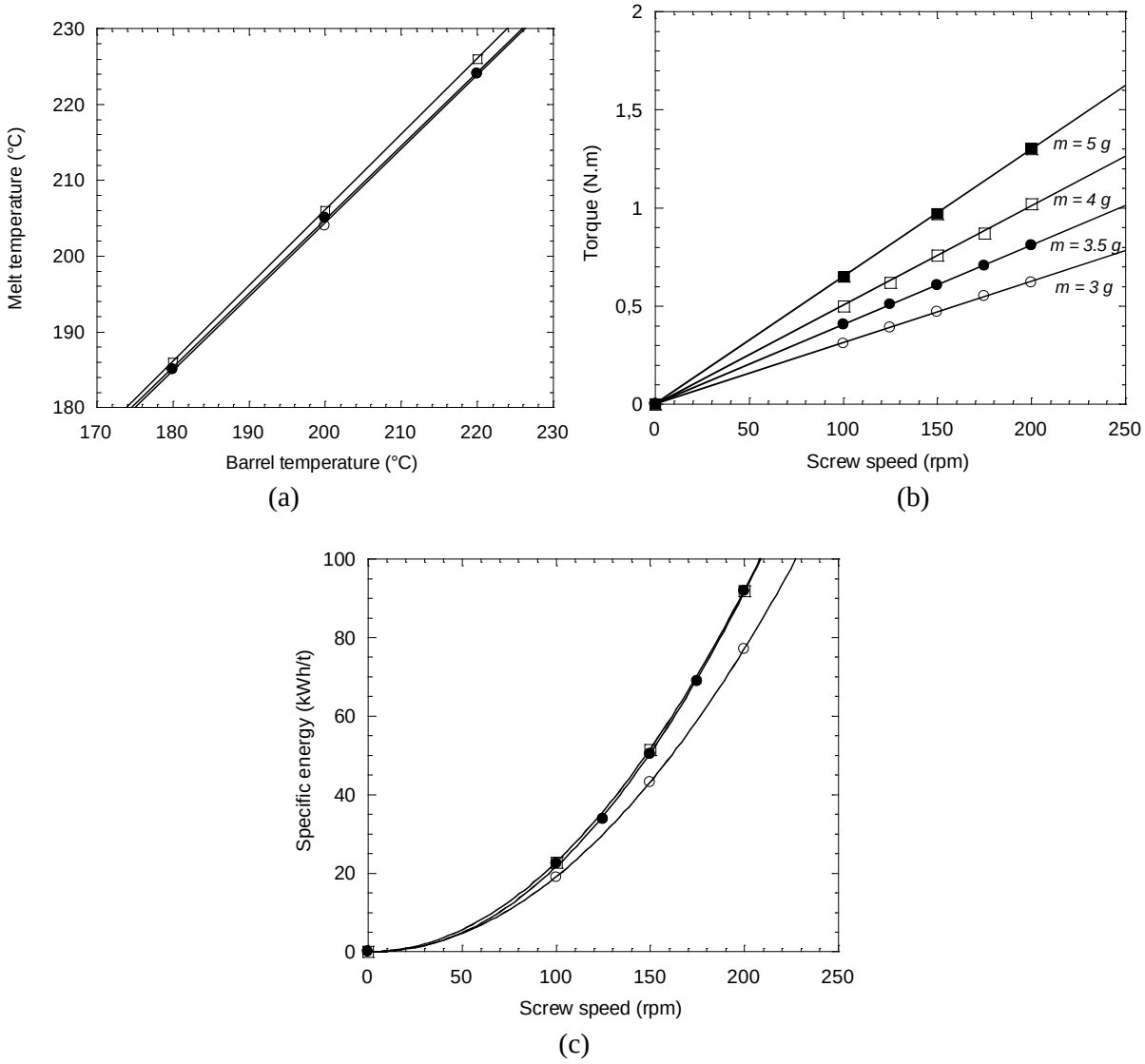


Figure 2. (a) Change in melt temperature with barrel temperature, for various screw speeds (○: 100 rpm, ●: 150 rpm, □: 200 rpm). (b) Change in torque with screw speed, for various feed masses at 180°C (○: 3 g, ●: 3.5 g, □: 4 g, ■: 5g). (c) Change in specific energy (for one minute of recirculation)

with screw speed, for various feed masses at 180°C (○: 3 g, ●: 4 g, □: 5 g). Lines are fits of the experimental points by linear or polynomial expressions.

It shows that the thermal regulation is very efficient, mainly due to the large surface of contact between the polymer and the micro-compounder, and the low thickness of the flow channels. Whatever the screw speed, the melt temperature is about 5°C higher than that of the barrel.

### *2.2.2 Torque*

The torque increases linearly with the screw speed (Figure 2b). It is also proportional to the mass introduced in the micro-compounder. As it is related to the viscosity, it decreases with the barrel temperature, for example from 1.04 to 0.79 N.m between 180 and 220°C, for $m$ = 4 g.

### *2.2.3 Specific mechanical energy*

The energy consumed during the process is directly provided by the software. It is obtained from the torque and the screw speed. To compare various situations, the specific mechanical energy (SME) is calculated from the energy dissipated during one minute of recirculation, divided by the feed mass. Figure 2c shows that SME varies as the square of the screw speed. It is quite independent of the feed mass and decreases slightly with the temperature (not shown). The order of magnitude is similar to those encountered in usual extrusion processes: for example, depending on processing conditions, Carneiro et al. [17] measured SME between 170 and 370 kWh/t on a Leistritz extruder (34 mm in diameter), and Berzin et al. [18] reported values in the range 200-800 kWh/t on a Clextral extruder (25 mm in diameter). Our values are also in agreement with those reported by Decaen et al. [13] for thermoplastic starch extruded on the same type of micro-compounder: 125 kWh/t at 100 rpm during 5 min, corresponding to 25 kWh/t for 1 min, which is what we can see in Figure 2c.

### *2.2.4 Pressure*

The pressures measured by the two sensors located in the recirculating channel theoretically allows to estimate the viscosity of the melt. Figure 3a shows an example of result, for two different feed masses. For a fixed mass, the pressure increases with the screw speed according

to a power law. At a fixed screw speed, it increases largely with the feed mass and decreases with the temperature (not shown). It means that the flow rate is highly dependent on the feed mass and not only on the screw speed, as generally admitted.

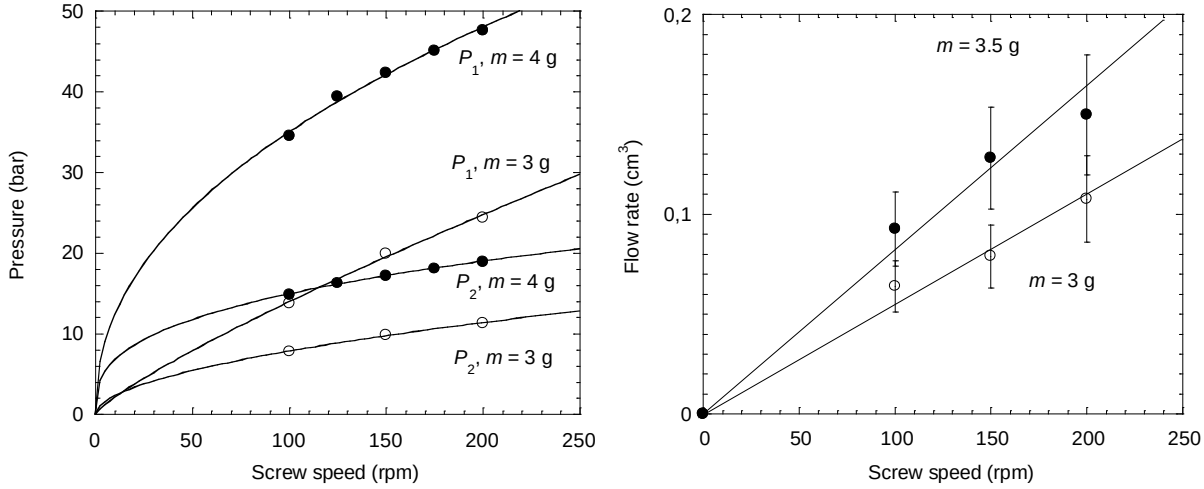


Figure 3. (a) Change in pressures $P_1$ and $P_2$ with screw speed, for various feed masses at 180°C (○: 3 g, ●: 4 g). Lines are fits of the experimental points by a power law. (b) Change in flow rate with screw speed, for various feed masses at 200°C (○: 3 g, ●: 3.5 g).

### *2.2.5 Flow rate*

The quantification of the flow rate is essential, among other for the determination of the viscosity. It has been measured by weighing the quantity of polymer extruded during the purge for 10 s. This mass flow rate is then converted into volume flow rate by dividing it by the melt density. Despite a certain dispersion of the values, it appears clearly that the flow rate is proportional to the screw speed (Figure 3b). However, as said in the previous paragraph, it depends also strongly on the feed mass: a change of 0.5 g (+ 16.6%) induces an increase of more than 60% of the flow rate. To our knowledge, it is the first time that this effect is reported. At fixed feed mass, the flow rate decreases slightly with the temperature (not shown), contrarily to the results of Yousfi et al. [12], which were obtained in a counter-rotating configuration. Anyway, for the various conditions we tested, coefficients $C$ (see Eq. (1)) in the range 5 $10^{-4}$ –

7.7 $10^{-4}$ were obtained, in good agreement with the values proposed by Yousfi et al. (5.5 $10^{-4}$ – 10.7 $10^{-4}$).

## 3 THEORETICAL MODEL

The objective of this section is to build a simplified one-dimensional model of the flow in the micro-compounder, based on the classical assumptions already used in single and twin-screw extrusion. [19, 20]

### 3.1 Flow geometry

#### *3.1.1 Twin-screw extruder*

We consider the geometry of a Haake Minilab© micro-compounder in a co-rotating configuration, as shown in Figure 1. The internal ($D_i$) and external ($D_e$) diameters of the screws decrease linearly along the axis *Z*. Consequently, the channel depth decreases also linearly with *Z*. The pitch *B* is constant, therefore the flight angle $\theta$ varies with *Z*:

$$\tan\theta(Z) = \frac{B}{\pi D_e(Z)} \tag{3}$$

For the Haake MiniLab©, $\theta$ thus increases from 30° to 58° along the screw.

We assume the classical hypotheses for calculating the flow along the screw channel, i.e. the screw geometry is unrolled and the barrel is moving at a relative velocity $V_b$ with respect to the screw [19, 20], the component of which in the channel direction can be written:

$$V_b(Z) = \frac{\pi N}{60} D_e(Z)\cos\theta(Z) \tag{4}$$

where the screw speed *N* is expressed in rpm. In first approximation, the channel section is considered as rectangular, with depth *H* and width *W* decreasing with *Z*:

$$W(Z) = \frac{B}{2}\cos\theta(Z) - e \tag{5}$$

where *e* is the flight thickness. The number 2 results from the fact that the screws are two-flighted. [21]

As the flight angle $\theta$ varies with $Z$, the unrolling of the channel is not trivial because the direction of the channel axis $z$ also varies, leading to a curved geometry (Figure 4). An increase of $dZ$ along the screw axis corresponds to an increase of $dz$ along the channel axis such as:

$$dz = \frac{dZ}{\sin\theta(Z)} \tag{6}$$

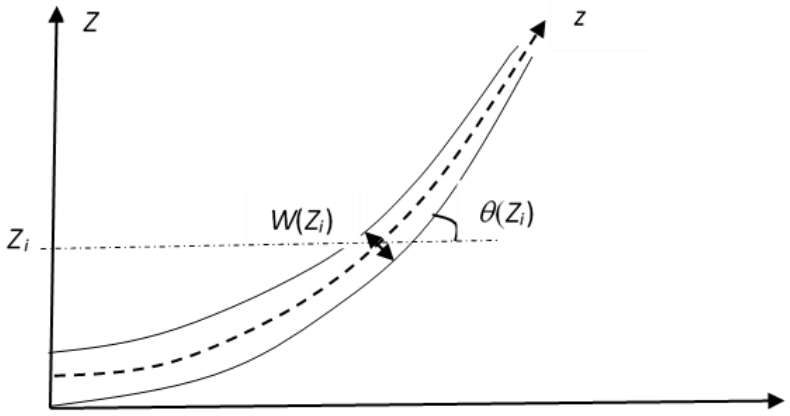


Figure 4. Geometry of the unrolled screw channel.

The free volume between the screws and the barrel can be estimated by considering that the screws are self-wiping and that their geometry can be described by the expressions proposed by Booy [22], except that the centerline distance and the sections of the screws and the barrel vary with $Z$. The calculations are given in Appendix. With the values given in Table 1, we obtain a total free volume $V_{screw}$ of 4.48 $cm^3$.

### *3.1.2 Recirculating channel*

A schematic view of the channel is shown in Figure 5 and the main dimensions are given in Table 1. Its volume $V_{channel}$ is calculated as 1.64 $cm^3$, i.e. approximately three times lower than the extruder one. The total internal volume of the micro-compounder is thus $V_{total} = V_{screw} + V_{channel}$ = 6.12 $cm^3$, in agreement with the value of 7 mL provided by Haake. For the PP used in the experiments, the maximum feeding mass is $m_{max} = \rho V_{total}$ = 4.5 g.

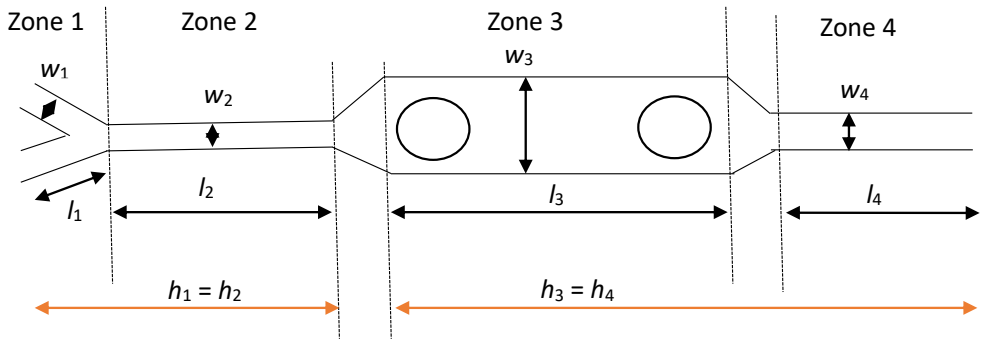


Figure 5. Schematics of the recirculating channel.

### 3.2 Operation of the micro-compounder

The micro-compounder does not work with an imposed flow rate, what makes its operation different from usual twin-screw extrusion systems. In the recirculation mode, only the screw speed and the feed mass are imposed. The flow rate results from the equilibrium between the pressure created by the screws and that consumed in the recirculating channel. This equilibrium also controls the residence time and thus the number of cycles supported by the material during the recirculation. During a cycle, the channel is always completely filled while the screws may be only partially filled. In this case, the screw filled volume and the axial filled length are called $V_{fill}$ and $L_{fill}$, respectively. In the partially filled section, the quantity of polymer is very low and can be neglected. Therefore, the filled volume in the screws can be expressed as:

$$V_{fill} = \frac{m}{\rho} - V_{channel} \tag{7}$$

where $m$ is the feed mass and $\rho$ the melt density.

The filled volume can also be calculated as:

$$V_{fill} = \int_{L-L_{fill}}^{L} S_f(Z)dZ \tag{8}$$

where $S_f$ is the free cross section between screws and barrel (see Appendix). The relationship between $V_{fill}$ and $L_{fill}$ is shown in Figure 6. From the feed mass, the filled volume is calculated from Eq. (7) and then the filled length from Eq. (8). For a filled length equal to $L_{max}$, Figure 6

shows that the filled screw volume is around 3 $cm^3$, i.e. a total volume of 4.6 $cm^3$, corresponding to 3.4 g for the selected PP.

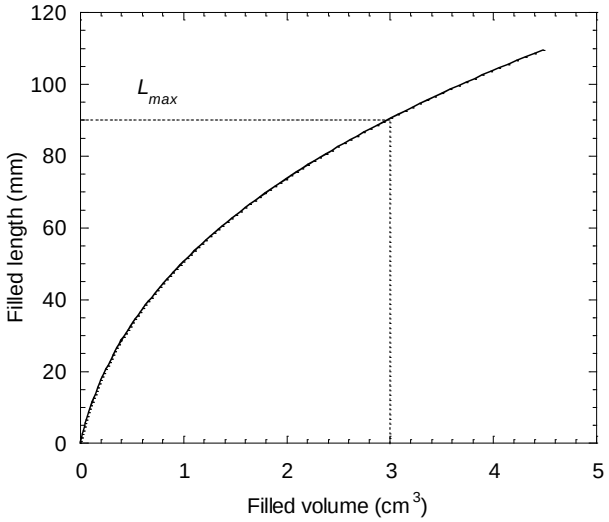


Figure 6. Filled length as function of filled volume for the screws.

### 3.3 Flow model

In a first step, a Newtonian fluid of viscosity $\eta$ is considered in isothermal conditions. Indeed, it has been shown in Figure 2a that the melt temperature is quite independent of the screw speed and very close to the barrel temperature. It can be explained by the large barrel surface in contact with the polymer and the low thickness of the channels, making the thermal regulation very efficient. We are only interested in the steady state flow during the recirculation of the molten polymer. The objective is to calculate the volume flow rate *Q* resulting from the equilibrium between the flows in the screws and in the channel.

#### *3.3.1 Flow along the channel*

The channel is constituted by a succession of four zones of constant rectangular cross-sections, and two short converging and diverging zones which can be neglected in a first approximation. For the four zones, the shear rate $\dot{\gamma}$, the pressure drop $\Delta p$ and the average residence time $\bar{t}$ are easily calculated using the usual expressions of pressure driven flows [21]:

$$\dot{\gamma}_1 = \frac{3Q}{w_1 h_1^{\,2}},\ \Delta p_1 = \frac{6\eta\, Q l_1}{w_1 h_1^{\,3}},\ \bar{t}_1 = \frac{2 w_1 h_1 l_1}{Q} \tag{9}$$

$$\dot{\gamma}_2 = \frac{6Q}{w_2 h_1^{\,2}},\ \Delta p_2 = \frac{12\eta\, Q l_2}{w_2 h_1^{\,3}},\ \bar{t}_2 = \frac{w_2 h_1 l_2}{Q} \tag{10}$$

$$\dot{\gamma}_3 = \frac{6Q}{w_3 h_3^{\,2}},\ \Delta p_3 = \frac{12\eta\, Q l_3}{w_3 h_3^{\,3}},\ \bar{t}_3 = \frac{w_3 h_3 l_3}{Q} \tag{11}$$

$$\dot{\gamma}_4 = \frac{6Q}{w_4 h_3^{\,2}},\ \Delta p_4 = \frac{12\eta\, Q l_4}{w_4 h_3^{\,3}},\ \bar{t}_4 = \frac{w_4 h_3 l_4}{Q} \tag{12}$$

The total pressure drop along the recirculating channel is thus:

$$\Delta p_{channel} = 12\eta\, Q\left[\frac{1}{h_1^{\,3}}\left(\frac{l_1}{2w_1}+\frac{l_2}{w_2}\right)+\frac{1}{h_3^{\,3}}\left(\frac{l_3}{w_3}+\frac{l_4}{w_4}\right)\right] \tag{13}$$

### *3.3.2 Flow along the screws*

As explained before, we consider the flow in a rectangular channel of decreasing cross-section. As the screws are two-flighted, the unrolled geometry consists in three parallel channels. [19] For the model, only one channel is considered, along which is flowing one third of the flow rate. [19] It can thus be written:

$$\frac{Q}{3} = \frac{V_b(Z)}{2}\frac{W(Z)H(Z)}{\alpha} - \frac{H(Z)^3}{12\eta}W(Z)\frac{dp}{dz} \tag{14}$$

where $V_b$ is the relative barrel velocity, defined by Eq. (4), and $z$ the direction of the curved channel (see Figure 4). The parameter $\alpha$ is introduced to express that the true cross section of the screw channel is lower than that of the rectangular channel. In the following, a value of 2 is selected for this parameter. The pressure gradient along $z$ can be deduced:

$$\frac{dp}{dz}(z) = \frac{12\eta}{W(Z)H(Z)^3}\left(\frac{V_b(Z)}{2}\frac{W(Z)H(Z)}{\alpha} - \frac{Q}{3}\right) \tag{15}$$

The pressure increase along the screws is thus:

$$\Delta p_{screw} = \int_{l-l_{fill}}^{l} \frac{12\eta}{W(Z)H(Z)^3}\left(\frac{V_b(Z)}{2}\frac{W(Z)H(Z)}{\alpha} - \frac{Q}{3}\right)dz \tag{16}$$

where $l$ and $l_{fill}$ are the equivalent of $L$ and $L_{fill}$ along the channel direction $z$.

In steady state recirculating conditions, $\Delta P_{screw} = \Delta P_{channel}$. This leads to:

$$Q\left[\frac{1}{h_1^3}\left(\frac{l_1}{2w_1}+\frac{l_2}{w_2}\right)+\frac{1}{h_3^3}\left(\frac{l_3}{w_3}+\frac{l_4}{w_4}\right)\right]=\int_{l-l_{fill}}^{l}\frac{1}{W(Z)H(Z)^3}\left(\frac{V_b(Z)}{2}\frac{W(Z)H(Z)}{\alpha}-\frac{Q}{3}\right)dz \quad (17)$$

The resolution of Eq. (17) will provide the value of the flow rate $Q$. However, a direct solution seems rather difficult and an iterative procedure can thus be proposed:

- for a fixed feed mass and screw speed, an initial value of $Q$ is estimated;
- $\Delta P_{channel}$ is calculated using Eq. (13);
- $(dp/dz)(Z)$ is calculated with Eq. (15), starting from the end of the screws ($Z = L$);
- the backward pressure is calculated as $P(z-1) = \Delta P_{channel} - \frac{dP}{dz}(Z)\,dz(Z)$;
- step by step, the procedure is repeated until $P = 0$ ;
- when $P = 0$, we must have $Z = L_{fill}$, as defined by Eqs. (7) and (8);
- if it is not the case, $Q$ is modified and the calculations are repeated until convergence.

### *3.3.3 Main flow parameters*

If we neglect the time spent in the partially filled section of the screws, the mean residence time for one recirculation cycle is:

$$\bar{t} = \frac{V_{channel} + V_{fill}}{Q} \quad (18)$$

This allows one to calculate the number of cycles $n$ for a fixed recirculation time $t_{rec}$:

$$n = \frac{t_{rec}}{\bar{t}} \quad (19)$$

The shear rates in the different sections of the channel are given by the equations (9) to (12). For the screws, the shear rate changes with the geometry and is more difficult to evaluate, as it is due to both screw speed and pressure gradient. In a previous study [23], it has been shown that the shear rate depends on the value of the maximum shear flow rate, defined as:

$$Q_{max}(Z) = \frac{3}{2} V_b(Z) \frac{W(Z)H(Z)}{\alpha} \tag{20}$$

If $Q(Z) < Q_{max}(Z)$:
$$\dot{\gamma}_{screw}(Z) = \frac{7}{4} \frac{V_b(Z)}{H(Z)} - \frac{Q}{W(Z)H(Z)^2} \tag{21}$$

If $Q(Z) > Q_{max}(Z)$:
$$\dot{\gamma}_{screw}(Z) = \frac{V_b(Z)}{4H(Z)} + \frac{Q}{W(Z)H(Z)^2} \tag{22}$$

The average strain in the channel can be defined as:

$$\Gamma_{channel} = \dot{\gamma}_1 \bar{t}_1 + \dot{\gamma}_2 \bar{t}_2 + \dot{\gamma}_3 \bar{t}_3 + \dot{\gamma}_4 \bar{t}_4 \tag{23}$$

where shear rates and mean residence times are given in Eqs. (9) to (12). For the screws, the local strain is approximated as $\dot{\gamma}_{screw}(Z)\bar{t}(Z)$, where the local average residence time is calculated as $\bar{t}(Z) = \frac{3H(Z)W(Z)dz}{\alpha Q}$. The average strain is thus:

$$\Gamma_{screw} = \sum_{l_{fill}} \frac{3H(Z)W(Z)\dot{\gamma}_{screw}(Z)\,dz}{\alpha Q} \tag{24}$$

The specific mechanical energy (SME) is calculated from the values of the shear rates. For the channel, we have:

$$SME_{channel} = \frac{\eta}{\rho Q}\left(2\dot{\gamma}_1^{\,2} h_1 w_1 l_1 + \dot{\gamma}_2^{\,2} h_2 w_2 l_2 + \dot{\gamma}_3^{\,2} h_3 w_3 l_3 + \dot{\gamma}_4^{\,2} h_4 w_4 l_4\right) \tag{25}$$

and for the screws:

$$SME_{screw} = \frac{3\eta}{\rho Q} \int_{l-l_{fill}}^{l} \frac{H(Z)W(Z)}{\alpha} \dot{\gamma}_{screw}^2(Z)\,dz \tag{26}$$

### 3.4 Non-Newtonian model

Until now, a constant viscosity has been considered. However, it is possible to generalize the previous model by taking into account an equivalent viscosity, function of the shear rate.

#### *3.4.1 Flow along the channel*

A value of the flow rate $Q$ has first to be chosen. It allows one to calculate the shear rates in the different sections (Eqs. (9) to (12)), and the corresponding viscosities ($\eta_1$, $\eta_2$, $\eta_3$, $\eta_4$) according

to the selected viscosity law (power-law, Carreau law…). The total pressure drop is then calculated as:

$$\Delta p_{channel} = 12\ Q\left[\frac{1}{h_1^3}\left(\frac{\eta_1 l_1}{2w_1}+\frac{\eta_2 l_2}{w_2}\right)+\frac{1}{h_3^3}\left(\frac{\eta_3 l_3}{w_3}+\frac{\eta_4 l_4}{w_4}\right)\right] \quad (27)$$

### *3.4.2 Flow along the screws*

As the shear rate varies with $Z$ (Eqs. (21) and (22)), the viscosity will also change along the screws. The expression of the pressure gradient is thus slightly modified:

$$\frac{dp}{dz}(z) = \frac{12\eta(Z)}{W(Z)H(Z)^3}\left(\frac{V_b(Z)}{2}\frac{W(Z)H(Z)}{\alpha}-\frac{Q}{3}\right) \quad (28)$$

As for the Newtonian case, the decrease of the pressure along the screws is calculated from the value of $\Delta p_{channel}$, until reaching $p = 0$. The value of $z$ for which $p = 0$ is then compared to the value of $l_{fill}$ corresponding to the feed mass (Eqs. (7) and (8)), and the value of $Q$ is modified accordingly. Once the iterative process is achieved, the final value of the flow rate allows one to calculate the SME for the channel and the screws:

$$SME_{channel} = \frac{1}{\rho Q}\left(2\eta_1 \dot{\gamma}_1^{\,2} h_1 w_1 l_1 + \eta_2 \dot{\gamma}_2^{\,2} h_2 w_2 l_2 + \eta_3 \dot{\gamma}_3^{\,2} h_3 w_3 l_3 + \eta_4 \dot{\gamma}_4^{\,2} h_4 w_4 l_4\right) \quad (29)$$

$$SME_{screw} = \frac{3}{\rho Q}\int_{l-l_{fill}}^{l} \eta(Z)\dot{\gamma}_{screw}^{\,2}(Z)\ \frac{H(Z)W(Z)}{\alpha}\,dz \quad (30)$$

## 4 RESULTS AND VALIDATION

In a first step, the main results of the non-Newtonian model are discussed. Then, the theoretical predictions are compared to the experiments presented in section 2.

### 4.1 Non-Newtonian model

We consider the case of 3 g of PP extruded at 200 rpm and 200°C. From Eqs. (7) and (8), a filled length $L_{fill}$ of 81 mm is calculated. The iterative procedure converges for a flow rate of 0.16 $cm^3/s$. The resulting pressure evolution is shown in Figure 7a. The pressure increases along the screws to reach a maximum at approximately 17 mm from the screw end, then decreases to

the end of the recirculating channel. The maximum pressure of 7.1 MPa is much larger than those measured along the recirculating channel, $P_1$ and $P_2$, respectively 4.0 and 1.4 MPa.

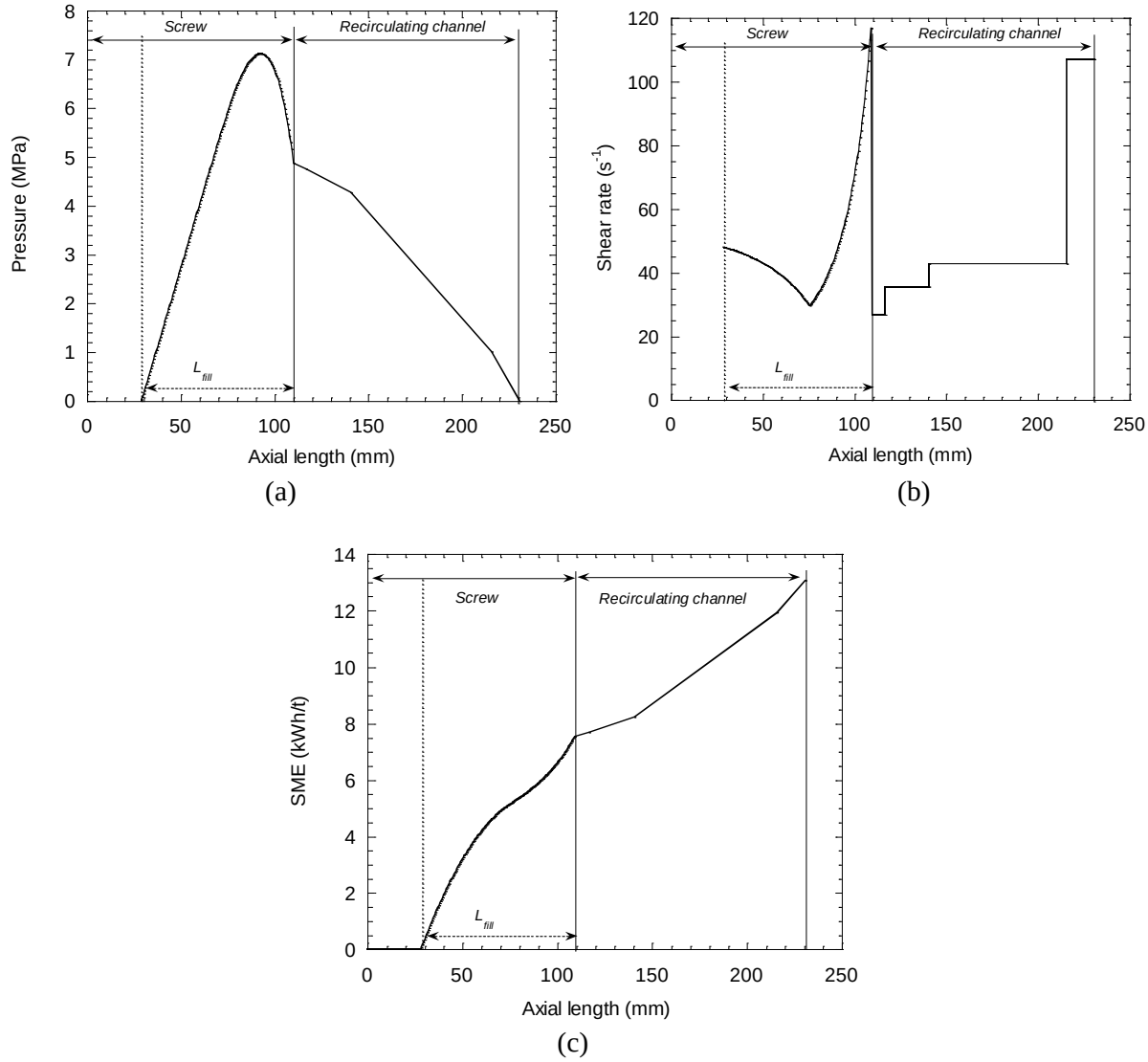


Figure 7. Change (a) in the pressure, (b) in the shear rate, and (c) in the specific mechanical energy along the screws and the recirculating channel ($m$ = 3 g, $N$ = 200 rpm, $T_b$ = 200°C)

The shear rates can be calculated from Eqs. (9)-(12) and (21)-(22). It can be seen in Figure 7b that they are very heterogeneous, but in the same range for the screws and the channel: they vary from 30 to 117 $s^{-1}$ in the screws and from 27 to 107 $s^{-1}$ in the recirculating channel. Therefore, if the Newtonian model would be able to provide correct qualitative results, it is however necessary to use the non-Newtonian one to obtain quantitative values.

The specific mechanical energy (*SME*) is an important parameter in extrusion. It is evaluated using Eqs. (29) and (30) and its evolution along the screws and the channel is presented in Figure 7c. The SME increases principally in the first and last parts of the screws, where the shear rates are high. The part dissipated in the screws (7.5 kWh/t) is comparable to that in the recirculating channel (5.5 kWh/t). For one cycle (in the present case, it lasts 25.4 s), the total SME is thus 13 kWh/t. As many cycles are usually involved in the process, the final SME is of the same order of magnitude as those encountered in pilot-scale or industrial extruders. On the same type of micro-compounder and for a formulation of starch plasticized with glycerol, Decaen et al. [13] measured a value of 123 kWh/t, for 300 s at 100 rpm, which corresponds to 10.4 kWh/t for a duration of 25.4 s. Even though material and screw speed are different, the order of magnitude remains the same.

The influence of the screw speed is shown in Figure 8a: when the screw speed is increased at constant feed mass, the filled length remains constant but the flow rate increases linearly. Consequently, the pressure increases also, as do the shear rates. In contrast, the residence time decreases, from 64.7 s at 100 rpm to 25.4 s at 200 rpm, for one cycle. At 150 rpm, a residence time between 1 and 2 min for one cycle was estimated by Chabrat et al. [24] on a plasticized starch, using a colored tracer.

Figure 8b show the effect of the feed mass. At constant screw speed and temperature, the filled length and the pressure level increase with the feed mass. A minimal feed mass of 1.2 g is necessary to fill the recirculating channel. Above this value, filled length and flow rate increase non-linearly with the mass, until reaching a total feeding of the screws for $m$ = 4.5 g (Figure 9). As already shown in the experiments, the flow rate during the recirculation is highly dependent on the feed mass.

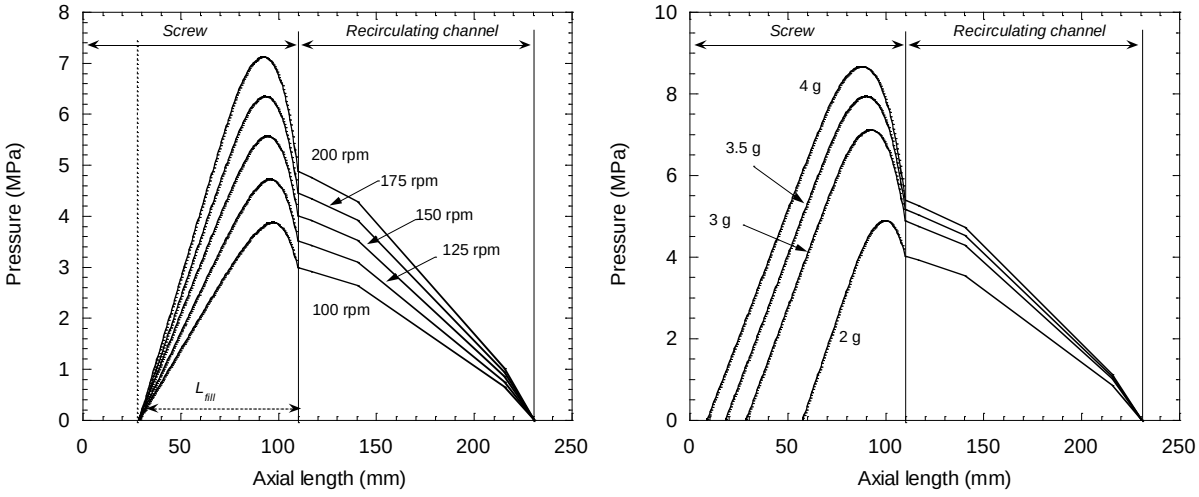


Figure 8. Change in the pressure along the screws and the recirculating channel, for various values (a) of screw speed ($m$ = 3 g, $T_b$ = 200°C) and (b) of feed mass ($N$ = 200 rpm, $T_b$ = 200°C)

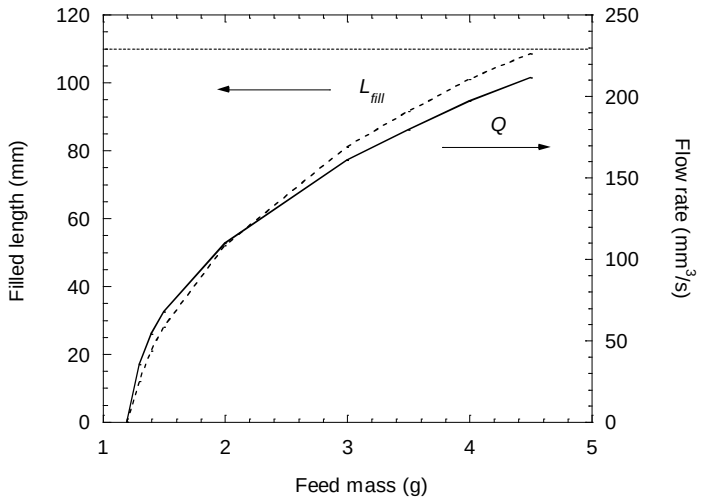


Figure 9. Change in the filled length (dotted line) and the flow rate (full line) with the feed mass ($N$ = 200 rpm, $T_b$ = 200°C)

As the filled volume and the flow rate increase simultaneously with the feed mass, the residence time is almost constant: at 200 rpm, between 2.0 and 4.5 g, it varies only from 24.5 to 28.5 s for one cycle.

The last parameter to evaluate is the barrel temperature. As the flow is considered as isothermal, only the viscosity of the fluid is impacted. Therefore, an increase in barrel temperature leads to a decrease of the pressure, at constant filled length (Figure 10) and a slight decrease of the flow

rate: at 200 rpm, from 0.162 $cm^3/s$ at 180°C to 0.161 $cm^3/s$ at 200°C and 0.160 $cm^3/s$ at 220°C. These results are in qualitative agreement with the experiments presented in section 2.2.5, but in contrast with the results of Yousfi et al. [12] who reported a slight increase in flow rate with temperature.

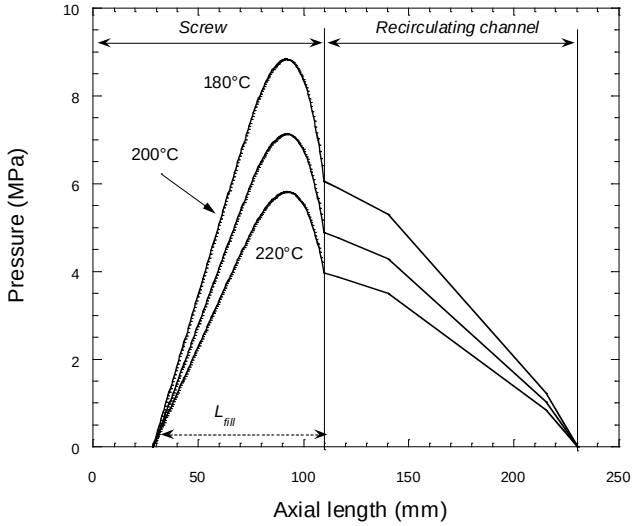


Figure 10. Change in the pressure along the screws and the recirculating channel, for three values of barrel temperature ($N$ = 200 rpm, $m$ = 3 g)

### 4.2 Experimental validation

Validations on pressure and flow rate have been made by using the non-Newtonian model. As an example, Figure 11 shows the change in the pressures $P_1$ and $P_2$ with the screw speed and the barrel temperature. The orders of magnitude are correctly predicted by the model, as well as the respective influences of speed and temperature. Generally speaking, these tendencies are observed for the different cases experimentally tested.

Figure 12 presents the validation of the flow rate for all measured conditions (various barrel temperatures, screw speeds and feed masses). This comparison must be made with caution for many reasons. First, the flow rate is not constant during the purge and only an average value can be estimated. Second, the flow conditions are different during the purge and the recirculation, because the flow channels are different and thus the resistance opposed to the

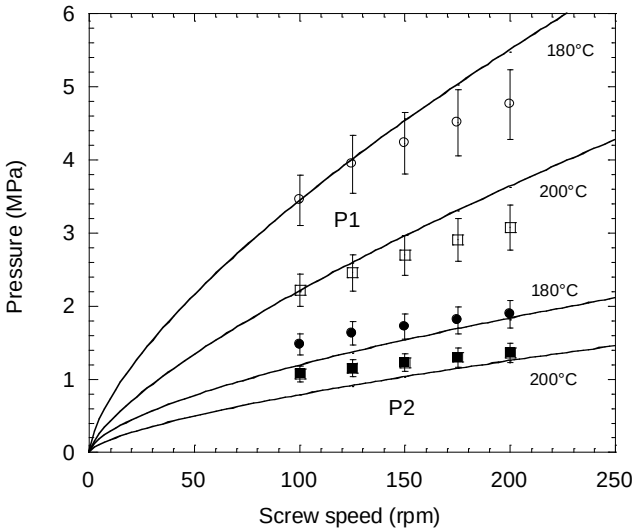


Figure 11. Change in the pressures $P_1$ and $P_2$ with the screws speed at two barrel temperatures. Comparison between model (full lines) and experiments (symbols) ($m$ = 4 g)

flow created by the screws. However, this is the only method that can be used to estimate the flow rate, as it was done previously by Yousfi et al.. [12] Once again, the model provides a satisfactory order of magnitude, whatever the flow conditions.

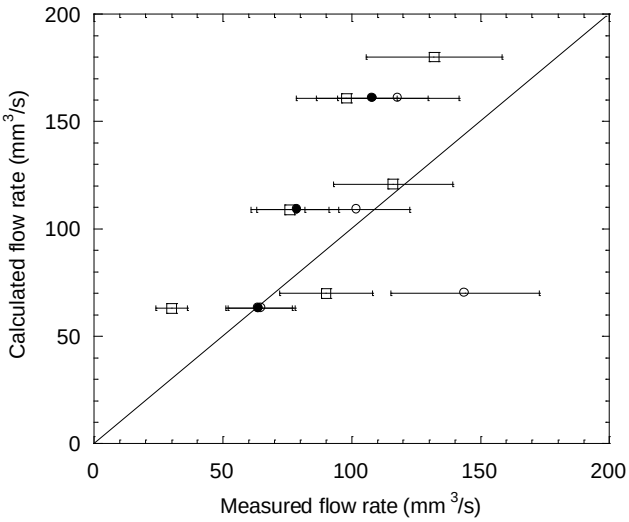


Figure 12. Comparison between calculated and measured values of the flow rate (○: $T_b$ = 180°C, ●: $T_b$ = 200°C, □: $T_b$ = 220°C)

Anyway, considering the approximations made and the simplicity of the approach (1D analytical), it can be concluded that the proposed model is able to provide satisfactory results and thus that it can be used for a better exploitation of the micro-compounders.

## 5 CONCLUSIONS

A model of the flow of a molten polymer in a micro-compounder equipped with two co-rotating conical screws has been established. Based on the usual approximations made in extrusion modelling, it allows to calculate for a non-Newtonian fluid the main parameters of the process, such as flow rates, pressures, residence times, specific energy, as function of screw speed, barrel temperature and feed mass. Experiments have shown that the flow rate is proportional to screw speed and depends largely on the feed mass, and only slightly on the temperature. The filling ratio is fixed by the feed mass and the melt temperature is controlled by the barrel regulation. In usual processing conditions, specific energy and residence times are close to those encountered on larger extruders. Finally, the comparison between theoretical and experimental results has shown that the main influences of the processing parameters are correctly predicted and that the order of magnitudes of pressures and flow rates are satisfactorily provided by the model.

## REFERENCES


[1] M. Marić, C.W. Macosko, *Polym. Eng. Sci*., **2001**, *41*, 118.

[2] A. Taguet, B. Otazaghine, M. Batistella, *Polymer*, **2020**, *191*, 122277.

[3] B. Fan, Y. Liu, D. He, J. Bai, *Materials*, **2017**, *10*, 838.

[4] U. Sundararaj, P. Pötschke, *Macromol. Mat. Eng*., **2006**, *291*, 227.

[5] F. Chavarria, R.K. Shah, D.L, D.R. Paul, *Polym. Eng. Sci*., **2007**, *47*, 1847.

[6] T. Li, K. Kuklisin, J. Auger, J. Nielsen, W. Lin, *Intern. Polym. Proc*., **2012**, *27*, 91.

[7] I. Ghebre-Sellassie, C.E. Martin, F. Zhang, J. DiNunzio, *Pharmaceutical Extrusion Technology*, 2018, CRC Press, Boca Raton (Fl).

[8] S.U. Schilling, N.H. Shah, A.W. Malick, J.W. McGinity, *Europ. J. Pharm. Biopharm*., **2010**, *74*, 352.

[9] G. Verstraete, J. Van Renterghem, P.J. Van Bockstal, S. Kasmi, B.G. De Geest, T. De Beer, J.P. Remon, C. Vervaet, *Intern. J. Pharm*., **2016**, *506*, 214.

[10] S. Guns, V. Mathot, J.A. Martens, G. Van den Mooter, *Europ. J. Pharm. Biopharm*., **2012**, *81*, 674.

[11] A. Almeida, L. Saerens, T. De Beer, J.P. Remon, C. Vervaet, *Intern. J. Pharm*., **2012**, *439*, 223.

[12] M. Yousfi, S. Alix, M. Lebeau, J. Soulestin, M.F. Lacrampe, P. Krawczak, *Polym. Test*., **2014**, *40*, 207.

[13] P. Decaen, A. Rolland-Sabaté, G. Colomines, S. Guilois, D. Lourdin, G. Della Valle, E. Leroy, *Carbohydr. Polym*., **2020**, *230*, 1.

[14] T. Sakai, M. Thommes, *J. Pharm. Pharmacol*., **2013**, *66*, 218.

[15] C. Wang, J. Wang, C. Yu, B. Wu, Y. Wang, W. Li, *Polym. Test*., **2014**, *33*, 138.

[16] C. Fernandes, A.J. Pontes, J.C. Viana, A. Gaspar-Cunha, *Polym. Eng. Sci*., **2010**, *50*, 1667.

[17] O.S. Carneiro, J.A. Covas, B. Vergnes, *J. Appl. Polym. Sci*., **2000**, *78*, 1419.

[18] F. Berzin, A. Tara, L. Tighzert, B. Vergnes, *Polym. Eng. Sci*., **2010**, *50*, 1758.

[19] P. G. Lafleur, B. Vergnes, *Polymer Extrusion*, **2014**, ISTE-Wiley, London.

[20] J.L. White, E.K. Kim, *Twin Screw Extrusion: Technology and Principle*, **2010**, Hanser, Munich.

[21] J.F. Agassant, P. Avenas, P.J. Carreau, B. Vergnes, M. Vincent, *Polymer Processing, Principles and Modelling*, **2017**, Hanser, Munich.

[22] M.L. Booy, *Polym. Eng. Sci*., **1978**, *18*, 973.

[23] B. Vergnes, *Polymers*, **2021**, *13*, 304.

[24] E. Chabrat, A. Rouilly, P. Evon, A. Longerias, L. Rigal, *PPS-26 Polymer Processing Society Annual Meeting*, **2010**, Banff, Canada.

**Appendix. Calculations of the geometry of the screws [22]**

The centerline distance varies linearly from $C_{l0}$ = 12 mm to $C_{l1}$ = 4.5 mm. The interpenetration angle $\psi$ is defined as:

$$\cos\psi(Z) = \frac{C_1(Z)}{D_e(Z)} \tag{A1}$$

and the flight angle by: $$\alpha(Z) = \frac{\pi}{2} - 2\psi(Z) \tag{A2}$$

because the screws have two flights.

The sections of the screw $S_s$ and the barrel $S_b$ are given by:

$$S_s(Z) = \left[\pi - \psi(Z)\right]\frac{D_e^2(Z)}{2} + \frac{C_l(Z)D_e(Z)}{2}\sin\psi(Z) \tag{A3}$$

$$S_b(Z) = 2\left[\psi(Z)C_1^2(Z) - \frac{C_1(Z)D_e(Z)}{2}\sin\psi(Z)\right] + \alpha(Z)\left[\frac{D_e^2(Z)}{4} + \left(C_1(Z) - \frac{D_e(Z)}{2}\right)^2\right] \tag{A4}$$

The free cross-section is thus given by:

$$S_f(Z) = S_b(Z) - 2S_s(Z) \tag{A5}$$

The total free volume is obtained by integration:

$$V_{screw} = \int_0^L S_f(Z)dZ \tag{A6}$$

If $L_{fill}$ is the length of the filled section of the extruder, the filled volume is given by:

$$V_{filled} = \int_{L-L_{fill}}^{L} S_f(Z)dZ \tag{A7}$$

## Graphical Abstract